PHYSICAL REVIEW C, VOLUME 63, 011601(R)

Fragment emission time from well defined sources in ^{58}Ni+^{197}Au at 34.5 MeV/nucleon

Zhi-Yong He,[1,*] L. Gingras,[1] Y. Larochelle,[1] D. Ouerdane,[1,†] L. Beaulieu,[1] P. Gagné,[1,‡] Xing Qian,[1,§] R. Roy,[1] C. St-Pierre,[1] G. C. Ball,[2,‖] and D. Horn[2]

[1]*Laboratoire de Physique Nucléaire, Département de Physique, Université Laval, Québec, Canada G1K 7P4*

[2]*AECL, Chalk River Laboratories, Ontario, Canada K0J 1J0*

(Received 12 July 2000; published 15 December 2000)

We have measured two-fragment correlation functions of the intermediate mass fragments emitted from quasiprojectile sources and midrapidity component formed in ^{58}Ni+^{197}Au at 34.5 MeV/nucleon. The two-fragment correlation functions of midrapidity component show a stronger Coulomb suppression than the quasiprojectile source. This Coulomb suppression for midrapidity component changes very little with the excitation energy of the quasiprojectile source deduced event by event by calorimetry method. By comparing the experimental correlation functions with an *N*-body Coulomb trajectory code calculation, the emission time of quasiprojectile sources has been extracted as a function of the excitation energy. The emission time decreases monotonically with the excitation energy in the range of 2–6 *A* MeV from 550 fm/c to about 150 fm/c. Above excitation energy of 6*A* MeV, the emission time becomes shorter and constant, suggesting that prompt multifragmentation occurs in these quasiprojectile sources.

DOI: 10.1103/PhysRevC.63.011601 PACS number(s): 25.70.Pq

A major objective of current heavy-ion collision studies at intermediate energy is to probe nuclear liquid-gas phase transition and multifragmentation [1]. Some experiments have been performed to try to find some signs and experimental evidence (e.g., [2–4]). Since fragments in heavy-ion collisions may come from various sources, source selection and source identification are important. Recently, experiments concentrated on the study of quasiprojectile (QP) source or projectile spectator. The projectile spectator from Au+Au collisions was employed by Pochodzalla *et al.* [2] to search for signals of a nuclear phase transition. The relation between the temperature and the excitation energy of a nuclear system (so-called caloric curve) exhibited a behavior which is expected for a phase transition. However, the nuclear caloric curve for the projectile spectator formed in the interaction of 1*A* GeV Au with C did not exhibit any evidence for a first order liquid-gas phase transition [3]. While the debate continues relative to these findings on nuclear caloric curve, negative heat capacity was observed in an excited QP source formed in Au + Au heavy systems at 35 MeV/nucleon, suggesting experimental evidence of the liquid-gas phase transition [4].

More recently a signal for transition from surface to bulk emission expected for spinodal decomposition was reported for the equilibriumlike sources formed in a hadron-induced collision, by studying the emission time as a function of the excitation energy [5]. In the past decade, intermediate mass fragment (IMF) emission time has been extracted in heavy-ion collisions from two-fragment correlation functions for various projectile-target combinations in a wide bombarding energy range [6–11]. The transition from long to short emission time has been deduced as a function of bombarding energy [6] and excitation energy which was estimated from projectile-target combination and bombarding energy [11]. Without an impact parameter neither source selection, only the averaged emission time over all sources, was deduced for these measurements. For example, in ^{84}Kr+^{93}Nb collisions at 35 MeV/nucleon, an averaged emission time of 400 fm/c was extracted for IMF's detected at polar angles ranging from 7° to 35°, suggesting that a sequential binary decay occurs [6]. On the other hand, a shorter emission time of 200 fm/c was derived from the ^{36}Ar+^{197}Au collision at 35 MeV/nucleon for IMF's detected between 16° and 31° [7].

In this Rapid Communication, we report on a study of IMF emission time from well defined sources in ^{58}Ni +^{197}Au at 34.5 MeV/nucleon. The results show a clear transition for QP source from long to short emission time as a function of QP excitation energy. However, the fragment emission time of the midrapidity component changes very slightly with QP excitation energy. We present experimental evidence which shows prompt multifragmentation of a highly excited QP source.

The experiment has been performed at TASCC facility of Chalk River Laboratories, with a beam of ^{58}Ni at 34.5 MeV/nucleon incident on a ^{197}Au target. The charged particles were detected in the CRL-Laval 4π array constituted by 144 detectors set in ten rings covering polar angles between 3.3° and 140°. The forward four rings covering angles between 3.3° and 24° are each made of 16 plastic phoswich detectors with detection thresholds of 7.5 (27.5) MeV/nucleon for element identification of $Z=1(28)$ particles. Between 24° and 46°, two rings of 16 CsI(Tl) crystals achieve isotopic resolution for $Z=1$ and 2 ions and element identification for Z

*On leave from Institute of Modern Physics, Chinese Academy of Sciences, Lanzhou 730000, China.

†Present address: Niels Bohr Institute, Blegdamsvej 17, DK-2100 Copenhagen, Denmark.

‡Present address: Services Conseils Systematix, 830 Ernest- Gagnon, Québec, Qc, Canada G1S 3R3.

§Present address: Softart Microsystems, Inc., 421 King St., N. Waterloo, ON, Canada N2J 4E4.

‖Present address: TRIUMF, 4004 Wesbrook Mall, Vancouver, B.C., Canada V6T 2A3.

$=3$ and 4 ions with thresholds ranging from 2 to 5 MeV/nucleon. The last four rings covering angles between 46° and 140° are each made of 12 CsI(Tl) crystals for isotopic resolution of $Z=1$ and 2 ions and element identification of $Z=3$ and 4 ions. The main trigger for event recording was a charged particle multiplicity of at least three particles. Details on detectors and energy calibration can be found in Refs. [12–14].

Since the array does not have a complete angular coverage and suffers from non-negligable energy thresholds, the first step in the event-by-event analysis is to select the ''well''-characterized event in which sufficient information has been obtained. The selection is to demand that the total detected charge of each event ΣZ is more than 25, i.e., 90% of the projectile charge. This requirement keeps the peripheral and midcentral collision events. Since heavy fragments with low energy cannot be detected by the array, the selection rejects all central events in which no projectilelike fragments were detected. The second step in the data analysis is to sort the events in terms of impact parameter. Two global variables related to the violence of the collision have been tried. The first one is the total charged particle multiplicity of the event and the second one the total absolute parallel momentum of the charged particles in the center-of-mass reference frame ($\Sigma|P_{||}^{\text{c.m.}}|$). Simulations indicate that $\Sigma|P_{||}^{\text{c.m.}}|$ is a better parameter of experimental centrality for our detection system [15].

To reconstruct the QP source, the events were sorted into several bins as a function of $\Sigma|P_{||}^{\text{c.m.}}|$. For each event, the heaviest fragment with $Z\geqslant 8$ in the event was used as the QP evaporation residue. For the events without a heavy fragment of $Z\geqslant 8$, the fastest fragment with a velocity larger than 0.9 of beam velocity was used as the QP residue. All the particles and fragments of each event were considered as originating from the QP source if they were emitted forward in the QP residue reference frame. To determine the origin of the backward emitted particles in the QP reference frame, the assumption of an isotropic emission has been made. They were attributed to the QP according to the probability deduced from the relative velocity distribution between a given particle and the residue [4,15]. This technique employed on an event-by-event basis enables the present two-particle correlation analysis for well-identified sources. The excitation energy of the QP source was deduced event by event by calorimetry method [2–4,15]. Then the rest of the particles for the system were attributed to the midrapidity and quasi-target emission. Because of the relatively high detector energy thresholds, these detected particles originate mainly from the midrapidity component. All the events without QP residue were not used in the analysis. By combining these data sets, we have access to 2×10^6 events for which $\sim 20\%$ contain two or more IMF's from the QP source.

In the QP reconstruction, we assumed that the velocity of the residue in the QP frame could be neglected. Filtered simulation from the GEMINI code [16] indicates that the residue velocity has a symmetric distribution centered on the source velocity. The FWHM (full width at half maximum) of the residue velocity distribution decreases with the increasing residue charge, from FWHM/$V_{source}=12\%$ at $Z_{residue}=8$ to 2% at $Z_{residue}=24$. Velocity fluctuations from these residue result in less than 10% fluctuation in excitation energy.

To study the emission time as a function of the excitation energy of QP source E^*_{QP}/A, all the events were sorted into six bins in terms of E^*_{QP}/A: $E^*_{QP}/A=2-4$, 4–5, 5–6, 6–7, 7–8, and $E^*_{QP}/A\geqslant 8$ MeV. At excitation energy below 2 MeV/nucleon, few events with two IMF's from QP source were observed. Emission time was derived from the intensity-interferometry technique, based on two-fragment reduced-velocity correlation function, defined [6–9] as

$$1+R(V_{red})=\frac{N_{corr}(V_{red})}{N_{uncorr}(V_{red})}. \tag{1}$$

$N_{corr}(V_{red})$ is the observed reduced-velocity distribution ($V_{red}=|V_1-V_2|/(Z_1+Z_2)^{1/2}$) for fragment pairs selected from the same event (coincidence distribution) and $N_{uncorr}(V_{red})$ is the reduced-velocity distribution for fragment pairs selected from mixed events (background distribution). For the results presented here, mixed events were obtained by randomly selecting each member of a fragment pair from different events with the same excitation energy range and from the same source.

Experimental excitation-energy-gated two-fragment correlation functions, integrated over all fragment pairs with element numbers $3\leqslant Z\leqslant 6$ from ^{58}Ni$+^{197}$Au collisions at 34.5 MeV/nucleon, are shown in Fig. 1. The top panel of Fig. 1 shows the correlation function for fragment pairs selected from QP source for high excitation energy range $E^*_{QP}/A=7-8$ MeV and low excitation energy range $E^*_{QP}/A=2-4$ MeV. Yield suppression at low V_{red}, due to the Coulomb interaction between fragments, increases with E^*/A. A compact source that quickly emits fragments results in stronger Coulomb interactions between the emitted fragments than a larger source that emits particles more slowly. Consequently, the observed trend of the yield suppression indicates that the emission time scale decreases with the increasing excitation energy. The bottom panel of Fig. 1 shows the correlation function for fragment pairs selected from the midrapidity component for $E^*_{QP}/A=7-8$ MeV and $E^*_{QP}/A=2-4$ MeV. In contrast with the QP source, Coulomb suppression at low V_{red} for the midrapidity component changes very slightly with E^*_{QP}/A, indicating that the IMF-IMF interaction process, as measured by the correlation function, is independent of the QP excitation energy. Comparing the top and bottom panels of Fig. 1, the two-fragment correlation functions of the midrapidity component show a stronger Coulomb suppression at low V_{red} than for the QP source, suggesting a shorter emission time for the midrapidity component than for the QP source.

The emission time scale of the QP source at various excitation energies is extracted by comparing the data with the simulation of the *N*-body Coulomb trajectory code of Glasmacher *et al.* [5,17,18]. This code considers the fragments to be emitted from the surface of the source. The fragment emission time t was assumed to have the probability distribution $P(t)\sim e^{-t/\tau}$, where τ is the emission time of the

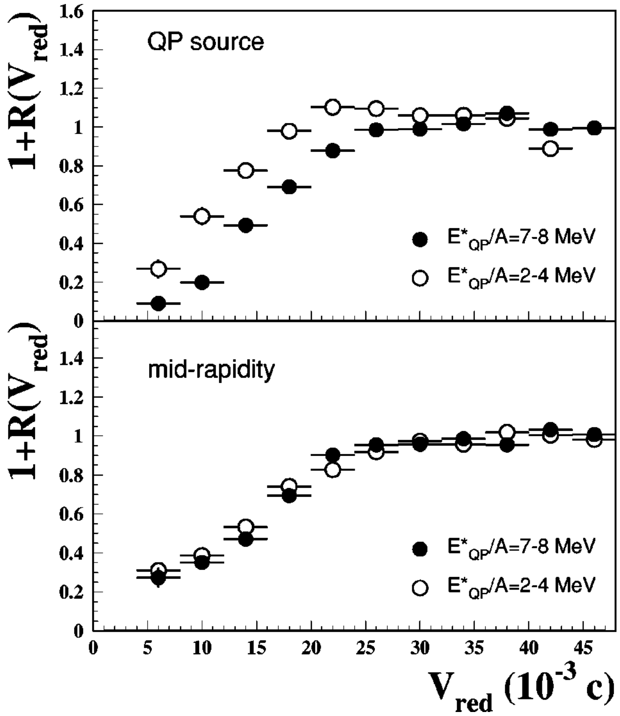

FIG. 1. Two-fragment correlation functions, integrated over all fragment pairs with element numbers $3 \leqslant Z \leqslant 6$ from quasiprojectile source (top panel) and midrapidity component and quasitarget sources (bottom panel), for ^{58}Ni+^{197}Au collision at 34.5A MeV. The open circles (full circles) are for $E^*_{QP}/A = 2-4$ $(7-8)$ MeV. The horizontal bars show the corresponding span in reduced velocity.

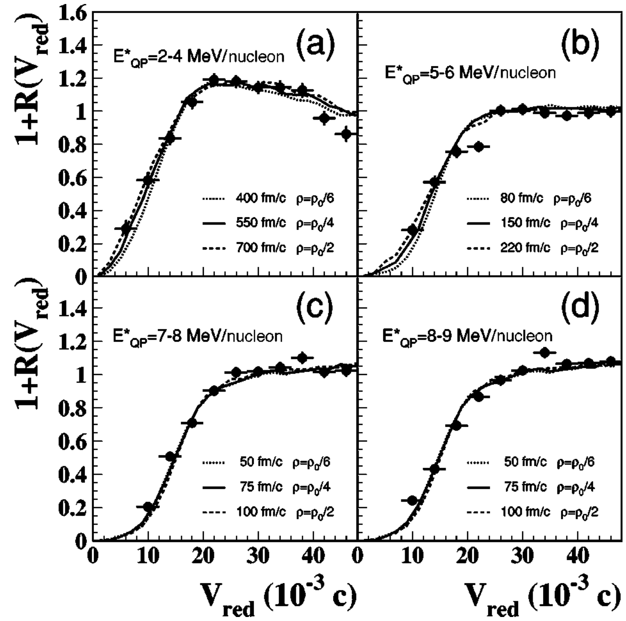

FIG. 2. As in Fig. 1, but for fragment pairs from quasiprojectile source, gated on excitation energy $E^*_{QP}/A = 2-4$ MeV (a), $5-6$ MeV (b), $7-8$ MeV (c), and $8-9$ MeV (d). The solid, dashed, and dot-dashed curves represent calculated correlation functions of a Coulomb trajectory calculation for fit parameters indicated on the figure. Statistical errors are shown as vertical bars.

source. The centers of the fragments were initially placed at a distance $R = R_S + R_{IMF} = rA_S^{1/3} + 1.2\ A_{IMF}^{1/3}$ from the center of the source, where r, $A_S^{1/3}$, and $A_{IMF}^{1/3}$ are the nuclear radius parameter, the mass of source, and the mass of fragment, respectively. The mass, charge, and energy of fragments were generated by randomly sampling the experimental yield distributions. After each emission, charge and mass of the emitted fragments were subtracted from the source. Because the charge, mass, and velocity of the starting source as well as the final residue are known from the experiments, no empirical adjustments of these quantities are required. Therefore, there are only two adjustable parameters in the simulation: emission time τ and nuclear radius parameter r (or nuclear density ρ). To better extract the emission time τ, we try a large range of source sizes, from $r = 1.54$ fm to $r = 2.22$ fm. This range for nuclear radius parameter r corresponds to a nuclear density range of $\rho = \rho_0/2 - \rho_0/6$ $(\rho = \rho_0/1.44 - \rho_0/4)$ using $r_0 = 1.22$ fm (1.44 fm) as a normal nuclear radius parameter. We only perform these simulations for a well-defined QP source to extract their emission time. Since the midrapidity component and quasitarget sources were not detected completely and not defined well in the experiment, we did not perform simulations for those sources.

In Fig. 2 we show fits to the correlation functions of the QP source for four bins in E^*_{QP}/A for a range of nuclear density ρ and emission time τ that yield minimum chi-squared values. Figures 2(a) and 2(b) show correlation functions for the lowest bin $E^*_{QP}/A = 2-4$ MeV and medium bin $E^*_{QP}/A = 5-6$ MeV, respectively. At the lowest E^*_{QP}/A bin, a very long emission time of about 550 fm/c was extracted, indicating that the QP source emits fragment by sequential binary disassembly. As the excitation energy raises from 2 MeV/nucleon to 6 MeV/nucleon, the emission time decreases monotonically from 550 fm/c to about 150 fm/c. Figures 2(c) and 2(d) show correlation functions for the highest two bins $E^*_{QP}/A = 7-8$ MeV and $E^*_{QP}/A = 8-9$ MeV, respectively. At high excitation energy, the emission time of the QP source becomes very short (~ 100 fm/c) and is independent of the excitation energy. The observed low τ values for high excitation energies are consistent with those values ($\tau \sim 100$ fm/c) predicted for prompt multifragmentation decay which originates from bulk instabilities of nuclear matter at low density.

To better understand these events with short emission time, the upper panel of Fig. 3 shows the probability for a given observed IMF multiplicity from QP, N_{IMF}^{QP}, as a function of excitation energy per nucleon, uncorrected for the experimental detection efficiency. The events with two IMF's begin at about $E^*_{QP}/A = 2$ MeV. Below that excitation energy, QP sources decay mainly by evaporating light particles or one fragment. At $E^*_{QP}/A \geqslant 3$ MeV, the events with three or four fragments begin to occur. The yield ratio of the three-fragment events to two-fragment events and of the four-fragment events to three-fragment events are shown in the middle panel of Fig. 3, uncorrected for the detection efficiency. At the E^*_{QP}/A range between 3 and 6 MeV, both yield ratios increase with E^*_{QP}/A. Above $E^*_{QP}/A \geqslant 6$ MeV,

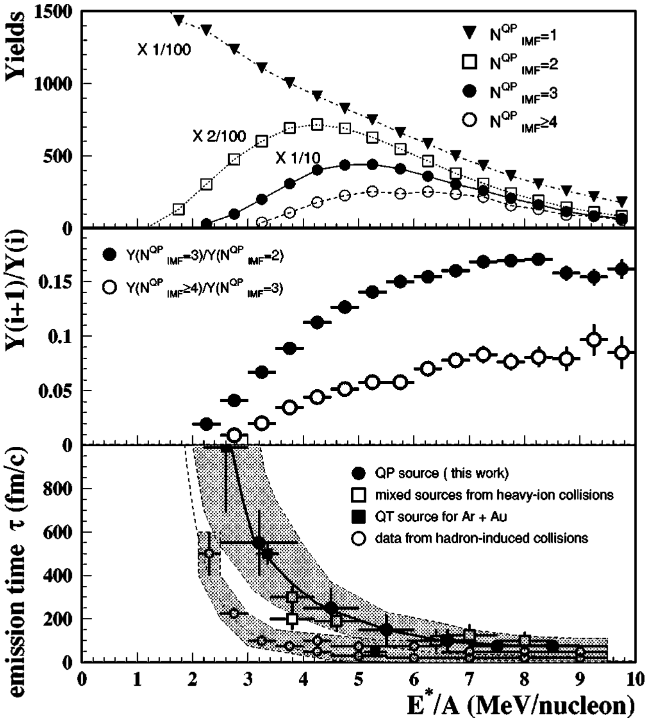

FIG. 3. Top: Dependence on the excitation energy per nucleon of QP source E^*_{QP}/A for the probability of observing a given multiplicity of IMF from QP source, uncorrected for the detection efficiency. Middle: Evolution of twofold vs threefold and threefold vs fourfold fragment prodution as a function of E^*_{QP}/A, uncorrected for the detection efficiency. Bottom: Emission time as a function of E^*_{QP}/A (full circles). The shaded area indicates the range of possible space-time solutions. The horizontal bars represent the excitation energy span and the vertical ones correspond to time ranges at a given excitation energy. The previous results for the QT source (solid squares) and mixed sources from heavy-ion collisions (open squares) [6–8,11,19,20], and heavy equilibriumlike sources formed in π^- and $p+{}^{197}$Au reaction (open circles) [5] are shown for comparison. The lines are used to guide the eye.

the yield ratios seem to saturate.

The solid circles in the bottom panel of Fig. 3 represent the averaged emission times for the QP source formed in Ni+Au collisions at 34.5 MeV/nucleon as a function of the excitation energy. The error bars shown in the figure reflect the space-time ambiguity of the correlation function. The shaded band shows the range of space-time values for which a consistent fit to all of the observables is achieved. A clear evolution of emission time from long to short values with excitation energy is observed. Above excitation energy of 6 MeV, the emission time becomes very short and constant. For these events with three and more fragments from QP, such a short emission time is interpreted as the evidence of prompt multifragmentation of the QP source in ^{58}Ni $+{}^{197}$Au collisions at 34.5 MeV/nucleon.

To compare with previous studies on emission time scale, the solid squares in the bottom panel of Fig. 3 show the emission times for the quasitarget (QT) source formed in Ar +Au collisions [19,20], while the open squares summarize the results for the mixed source of the QP and midrapidity contribution formed in Ar+Au, Ne+Au, and Kr+Nb collisions [6–8,11]. The excitation energy scale for these reactions was estimated by considering the target-projectile combination and the bombarding energy [11]. The open circles in the bottom panel of Fig. 3 come from a recent study on heavy equilibriumlike sources formed in π^- and $p+{}^{197}$Au reactions in which the excitation energy was deduced by a calorimetry method [5]. The emission time scale extracted for heavy equilibriumlike sources from hadron-induced reactions are systematically lower at low E^*/A compared to the present work. The deduced emission times saturate around 5–6 A MeV in the case of Ref. [5] while, in the present case, the saturation occurs at about 6A MeV for the QP source. The reaction mechanism might affect the emission time since in hadron-induced reactions there is very little rotation, deformation, or expansion involved.

In summary, two-fragment reduced-velocity correlation functions of the intermediate mass fragments emitted from quasiprojectile source and midrapidity component formed in ^{58}Ni$+{}^{197}$Au at 34.5A MeV have been studied in the excitation energy range of $E^*_{QP}/A=2-9$ MeV. The two-fragment correlation functions of the midrapidity component show a stronger Coulomb suppression at low V_{red} than for the QP source, suggesting a shorter emission time for the midrapidity component than QP source. But this Coulomb suppression at low V_{red} for the midrapidity component changes very little with E^*_{QP}/A, suggesting that their averaged emission time is independent of the excitation energy of the QP source. For the QP source, the two-fragment production is negligible at low excitation energies $E^*_{QP}/A \leqslant 2$ MeV, while the multifragment production begins to occur at $E^*_{QP}/A \geqslant 3$ MeV. Comparing the experimental correlation functions with the N-body Coulomb trajectory code calculations, the emission time scale of the QP source was extracted as a function of the excitation energy. The emission time decreases monotonically with the excitation energy in the range of 2–6 A MeV from 550 fm/c to 150 fm/c. Above excitation energy of 6A MeV, it becomes very short and constant, suggesting that the prompt multifragmentation occurs in these quasiprojectile sources.

The authors would like to thank Thomas Glasmacher for providing his N-body Coulomb trajectory code. This work was supported in part by the Natural Sciences and Engineering Research Council of Canada and the Fonds pour la Formation de Chercheurs et l'Aide à la Recherche du Québec.

[1] L. G. Moretto and G. J. Wozniak, Annu. Rev. Nucl. Part. Sci. **43**, 379 (1993); W. G. Lynch, *ibid.* **37**, 493 (1987), and references therein.
[2] J. Pochodzalla *et al.*, Phys. Rev. Lett. **75**, 1040 (1995).
[3] J.A. Hauger *et al.*, Phys. Rev. Lett. **77**, 235 (1996).
[4] M. D'Agostino *et al.*, Phys. Lett. B **473**, 219 (2000).
[5] L. Beaulieu *et al.*, Phys. Rev. Lett. **84**, 5971 (2000).
[6] E. Bauge *et al.*, Phys. Rev. Lett. **70**, 3705 (1993).

[7] Y. D. Kim *et al.*, Phys. Rev. Lett. **67**, 14 (1991); Phys. Rev. C **45**, 338 (1992).

[8] D. Fox *et al.*, Phys. Rev. C **47**, R421 (1993); **50**, 2424 (1994).

[9] D. R. Bowman *et al.*, Phys. Rev. Lett. **70**, 3534 (1993); Phys. Rev. C **52**, 818 (1995).

[10] Zhi Yong He *et al.*, Nucl. Phys. **A620**, 214 (1997); Phys. Rev. C **57**, 1824 (1998).

[11] D. Durand, Nucl. Phys. **A630**, 52c (1998), and references therein.

[12] Y. Larochelle *et al.*, Nucl. Instrum. Methods Phys. Res. A **348**, 167 (1994).

[13] D. Fox *et al.*, Nucl. Instrum. Methods Phys. Res. A **374**, 63 (1996).

[14] L. Gingras, Master degree thesis, Université Laval, 1998.

[15] L. Gingras *et al.*, XXXVI International Winter Meeting on Nuclear Physics, Bormio, Italy, 1998, p. 365.

[16] R. J. Charity *et al.*, Nucl. Phys. **A483**, 371 (1988).

[17] T. Glasmacher *et al.*, Phys. Rev. C **50**, 952 (1994).

[18] R. Popescu *et al.*, Phys. Rev. C **58**, 270 (1998).

[19] H.-Y. Wu *et al.*, Phys. Rev. C **57**, 3178 (1998).

[20] M. Louvel *et al.*, Phys. Lett. B **320**, 221 (1994).